WDM FSO Network With Turbulence-Accentuated Interchannel Crosstalk

Abisayo O. Aladeloba, Malcolm S. Woolfson, and Andrew J. Phillips

***Abstract*—A wavelength division multiplexing (WDM) access network using high-speed free-space optical (FSO) communication for the distribution link is proposed. Combining FSO communication with optical fiber can reduce the system cost and provide high-bandwidth access in regions where optical fiber installation is problematic. The WDM channels suffer from interchannel crosstalk, while the FSO communication performance in a clear atmosphere is limited by atmospherically induced scintillation. These impairments, plus the amplified spontaneous emission noise from optical amplification, combine in a potentially problematic way, particularly in the upstream direction, which is investigated here. This turbulence-accentuated crosstalk effect is considered for the cases of 1) signal turbulent but crosstalk not and 2) crosstalk turbulent but signal not. Error floors are obtained in each case. The FSO link length that can be supported in the general case of the hybrid network is investigated.**

***Index Terms*—Amplified spontaneous emission; Atmospheric turbulence; Fiber and free-space optical communications; Interchannel crosstalk; Wavelength division multiplexing.**

I. Introduction

Over the years, there has been an exponential rise in the demand for broadband applications and services [1,2]. Optical carrier technologies can be a good solution for the access networks, since they potentially offer huge bandwidth [2–6]. Passive optical networks (PONs) are the main contenders for optical access networks and have gradually replaced the copper-based access network technologies. Optical fiber has many advantages (low cost, no electromagnetic interference problems, and less power loss) over the incumbent copper systems [7,8]. At the moment, time division multiplexing/time division multiple access (TDM/TDMA) systems are the most popular architecture for PONs, although they are only suitable for a limited number of optical network units (ONUs) (unless augmented by optical amplification [9]) and they typically use power splitters. Wavelength division multiplexing (WDM) systems allow more ONUs to be connected at high data rates and assign a distinct pair of dedicated wavelengths to each ONU to establish a point-to-point connection between the ONU and the optical line terminator (OLT) [1]. Major drivers for the WDM PON are this potential bandwidth increase and the greater data security compared to the TDM/TDMA system [1,2,10–12].

Free-space optical (FSO) communication has been successfully applied for short-distance links (up to 4 km [5]). Relative to fiber systems, FSO communication has the advantage of ease of setup and tear down, provision of access in difficult locations, and lower cost (i.e., no purchasing and installing of fiber) [13–16]. FSO communication-based systems have advantages over RF (or millimeter-wave) systems such as improved security, no spectrum licensing, and faster speed over the short-haul access [4,5]. Nevertheless FSO communication is faced with considerable challenges such as atmospheric attenuation and turbulence-induced scintillation [4,5,7,14,17,18]. A WDM access network using FSO communication in the distribution link is a realistic proposition, since both fiber and FSO systems use similar transmission wavelengths and system components [10,19]. Therefore, the integration of both technologies may yield a cost effective and reliable hybrid optical access network solution.

For long FSO propagation distances optical amplifiers (OAs) are necessary. This is at the cost of amplified spontaneous emission (ASE) noise, which complicates performance calculations [20–22]. Optical amplification for extending the reach and/or split of fiber optical access networks (superPONs) was investigated in the 1990s [23], while WDM-based long-range PONs are now under investigation [9].

Interchannel crosstalk in WDM systems is well reported [8,24]. Here the situation changes as atmospheric turbulence in the hybrid network's distribution link causes a fluctuating crosstalk effect that significantly exacerbates its negative performance impact. The turbulence accentuation of interchannel crosstalk arises when the signal and crosstalk paths are independently turbulent (from being physically completely distinct, e.g., from different ONUs in the upstream) such that the crosstalk power may temporarily approach or even significantly exceed the signal power despite a sensible long-time average signal-to-crosstalk ratio. The probability of crosstalk power exceeding the signal power (either by turbulent increase of crosstalk or turbulent decrease of signal or both) provides an ultimate performance limit. Experimental work has demonstrated the feasibility of WDM FSO networks [10,25,26]. The effect of interchannel crosstalk has been investigated in [27] for an all-fiber TDM/WDM-PON with

Manuscript received January 25, 2013; revised April 19, 2013; accepted April 19, 2013; published May 31, 2013 (Doc. ID 183939).

The authors are with the Division of Electrical Systems and Optics, Faculty of Engineering, University of Nottingham, University Park, Nottingham NG7 2RD, UK (e-mail: andrew.phillips@nottingham.ac.uk).

http://dx.doi.org/10.1364/JOCN.5.000641

burst-mode reception at the OLT. However, the influence of turbulence-accentuated interchannel crosstalk on system performance has not been addressed previously and is thus the main focus here.

II. System Design and Description

Typically, a WDM PON connects a multiwavelength OLT to ONUs over an interconnecting fiber system. Figure 1 shows the proposed WDM PON using FSO communication instead of fiber for distribution links. The suboptimal performance of the remote node in the downstream transmission and the imperfection of the OLT demux in the upstream transmission lead to the reception of optical signals of undesired wavelengths, i.e., interchannel crosstalk. This effect is potentially more severe in the upstream, as it may be exacerbated by turbulence, while in the downstream the ONUs can typically be arranged so as to prevent the introduction of further crosstalk at the ONU photodiode (or an optical filter could optionally be placed before it). Note that (upstream) intrachannel crosstalk can also exist in principle if beam spreading leads to a fraction of the transmit power falling within the field of view of an unintended collecting lens. This is neglected here, as it can generally be avoided by ensuring that ONUs are not lined up to have near identical transmission paths.

A. Upstream Transmission

In the upstream, each ONU has a dedicated independent point-to-point optical link to the OLT with a laser of its own specific fixed wavelength. The distribution network (atmospheric channel) conveys the signals from the ONUs to a mux, which combines and transmits them through a single optical feeder fiber to the OLT. At the OLT the demux separates the multiplexed optical signals into constituent wavelengths. Several WDM mux/demux technologies exist. The arrayed waveguide grating (AWG)-based devices are

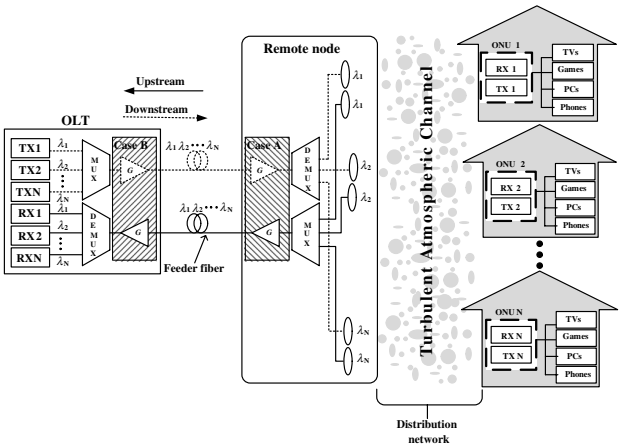

Fig. 1. Schematic representation of a WDM network using an FSO link for the final distribution stage, with an OA located at the remote node (Case A) or at the OLT demux input (Case B). ONUs will be distributed at different angles around the remote node.

very popular, mainly because of their low chromatic dispersion loss; however, production complexity and cost and temperature-dependent loss variation are drawbacks [1,8]. The free-space diffraction grating is a promising technology for overcoming the drawbacks of AWG-based and other older mux/demux devices [28]. For performance calculations it is assumed to have signal mux/demux loss L_{mux} and L_{demux} ($\leq$3.5 dB), adjacent channel additional loss $L_{\text{demux,adj}}$ (typically >30 dB), and non-adjacent-channel additional loss $L_{\text{demux,nonadj}}$ (typically >35 dB) [1,2,28]. The optical wavelengths are assumed to be in the C band (i.e., around 1550 nm) with channel spacing of 100 GHz [2] on the International Telecommunication Union Telecommunication Standardization Sector grid. This wavelength choice exploits low atmospheric and fiber attenuation and the suitability for an erbium-doped fiber amplifier and high-quality transmitters and receivers [3,8,22]. The ONU transmitters each transmit optical signals (on wavelengths $\lambda_1, \lambda_2, \ldots, \lambda_N$, where N is the number of ONUs connected to the network) toward corresponding receiver collecting lenses (RCLs) of diameter D_{RX} at the remote node. For the sake of definiteness, the ONU transmit power is assumed to not exceed 20 dBm, within the maximum possible value according to laser skin and eye safety regulations [29–31]. The FSO system transmitted powers typically exceed fiber PON ONU transmit powers both because the atmospheric channel is highly attenuating and because it lacks the nonlinear effects that occur in optical fiber. As it approaches the RCL, the beam spreads out, characterized by its divergence angle θ, due to diffraction and wave front distortion induced by atmospheric turbulence [32].

Each remote node RCL couples its wavelength through a short length of fiber (using a fiber collimator as in [20]) to the mux. An optical preamplifier of gain G and noise figure (NF) can be placed either at the remote node output to increase the signal power through the feeder fiber or at the demux input to improve the effective OLT receiver sensitivity. A PIN photodiode with quantum efficiency η is placed after the demux. The resulting electrical signal is then amplified and filtered before being passed to the decision device, where the threshold is applied. The photodetection process is a square law detection leading to signal-ASE and ASE–ASE beat noises. An integrate-and-dump receiver is assumed with electrical bandwidth $B_e = 1/2T_b$, where $T_b = 1/R_b$ and R_b is the data rate. The bit is sampled and compared with the threshold. For the on–off keyed (OOK) non-return-to-zero signaling assumed here, the Kalman filtering method [33] represents a realistic adaptive approach of achieving near optimal threshold for each instantaneous power level, and such an optimal threshold (however obtained) is assumed.

B. Downstream Transmission

In the downstream, N separate OLT lasers transmit signals belonging to each ONU on a particular wavelength in a point-to-point fashion. In the downstream performance calculations, the same assumptions as in the upstream are made for the optical wavelengths, channel spacing,

and use of optimal threshold in the OOK scheme. However, maximum OLT transmit powers are lower (typically 10 dBm [2]) to reduce fiber nonlinearity. Downstream interchannel crosstalk occurs due to imperfection of the remote node demux, but this is not accentuated by the atmospheric turbulence, since the crosstalk arises prior to the distribution link and so experiences essentially the same atmospheric link turbulence as the signal.

C. Optical Amplifier Placement

Two different amplifier locations are considered: Case A at the remote node and Case B at the OLT. In the upstream Case A, the ASE noise experiences loss due to feeder fiber attenuation and OLT demux loss, while in the upstream Case B, the ASE noise suffers from OLT demux loss only. In some cases the location of the upstream OA may not make much difference to the performance, considering that the optical signal-to-noise ratio (OSNR) differs by only about 4 dB between Case A and Case B (for 20 km fiber), which is not particularly significant when OSNR is good. Therefore, the upstream amplifier location choice may mainly depend on practical issues such as the availability of powering, at the remote node, which in turn depends on the powering of the pointing and tracking system, if needed. In the downstream Case A, the ASE noise suffers remote node demux loss, atmospheric attenuation, and beam spreading loss, while in the downstream Case B, the ASE noise additionally experiences feeder fiber attenuation. Similar issues to the upstream exist regarding amplifier placement, but with the additional need not to launch too much power into the fiber in the downstream Case B due to nonlinearity issues.

III. Turbulence Modeling

Atmospheric scintillation occurs due to thermally induced refractive index changes of the air along the optical link, causing rapid fluctuation of signal irradiance at the receiver, reduction in degree of coherence of the optical signal [34], and potentially poor bit error rate (BER). The gamma–gamma (GG) distribution is widely used for characterizing the whole range of turbulence effects, i.e., weak, moderate, and strong, not only because closed form expressions exist but also because of their direct dependence on turbulence parameters and the closeness to experimental results [14,17,35,36]. The GG probability density function (pdf) is given as [14,17,35,36]

$$p_{\mathrm{GG}}(h_X) = \frac{2(\alpha\beta)^{(\alpha+\beta)/2}}{\Gamma(\alpha)\Gamma(\beta)} h_X^{(\alpha+\beta)/2-1} K_{\alpha-\beta}\left(2\sqrt{\alpha\beta h_X}\right); \qquad h_X > 0, \tag{1}$$

where h_X is the attenuation due to atmospheric turbulence for the signal (h_{sig}) or interferer (h_{int}), α is the effective number of large-scale eddies of the scattering process, β is the effective number of small-scale eddies of the scattering process, $K_n(\cdot)$ is a modified Bessel function (second kind, order n), and $\Gamma(\cdot)$ is the gamma function. The signal and interferer travel over physically distinct paths in the upstream and thus have uncorrelated turbulence; hence, their GG pdfs are each treated independently. The α and β parameters for plane-wave propagation (for arbitrary aperture size) are given as [14,17,35,36]

$$\alpha = \left\{\exp\left[\frac{0.49\sigma_R^2}{(1+0.65d^2+1.11\sigma_R^{12/5})^{7/6}}\right]-1\right\}^{-1}, \tag{2}$$

$$\beta = \left\{\exp\left[\frac{0.51\sigma_R^2(1+0.69\sigma_R^{12/5})^{-5/6}}{1+0.9d^2+0.62d^2\sigma_R^{12/5}}\right]-1\right\}^{-1}, \tag{3}$$

where $d = \sqrt{kD_{RX}^2/4l_{\mathrm{fso}}}$ is the normalized RCL radius, $\sigma_R^2 = 1.23C_n^2k^{7/6}l_{\mathrm{fso}}^{11/6}$ is the Rytov variance, C_n^2 is the refractive index structure constant (ranging from $\approx 10^{-17}$ m$^{-2/3}$ to $\approx 10^{-13}$ m$^{-2/3}$), l_{fso} is the FSO link length, $k = 2\pi/\lambda$ is the wave number, and λ is the wavelength [14,17,35,36].

IV. General BER Analysis

In its most general form, under the assumption of independent signal and crosstalk channels (e.g., as in the upstream), the average (turbulence-accentuated) BER [for given fixed transmitter powers for the signal and crosstalk (the dependence on which is omitted below for brevity)] is

$$\overline{\mathrm{BER}} = \int_0^\infty \int_0^\infty \mathrm{BER}(h_{\mathrm{sig}}, h_{\mathrm{int}}) p_{\mathrm{GG,sig}}(h_{\mathrm{sig}}) \times p_{\mathrm{GG,int}}(h_{\mathrm{int}}) \mathrm{d}h_{\mathrm{sig}} \mathrm{d}h_{\mathrm{int}}, \tag{4}$$

where $p_{\mathrm{GG,sig}}(h_{\mathrm{sig}})$ and $p_{\mathrm{GG,int}}(h_{\mathrm{int}})$ are, respectively, the signal and interferer GG pdfs (each with different α, β, and σ_R^2). Treating the signal and interferer turbulent links as independent is meaningful in the upstream (as completely separate) but not in the downstream.

Using a Gaussian approximation, the BER (conditioned on h_{sig} and h_{int}) for (upstream) transmission with a single interchannel crosstalk wavelength is

$$\mathrm{BER}(h_{\mathrm{sig}}, h_{\mathrm{int}}) = \frac{1}{4}\mathrm{erfc}\left(\frac{Q(h_{\mathrm{sig}}, h_{\mathrm{int}})}{\sqrt{2}}\right), \tag{5}$$

$$Q(h_{\mathrm{sig}}, h_{\mathrm{int}}) = \frac{i_{1,0}(h_{\mathrm{sig}}, h_{\mathrm{int}}) - i_{0,1}(h_{\mathrm{sig}}, h_{\mathrm{int}})}{\sigma_{1,0}(h_{\mathrm{sig}}, h_{\mathrm{int}}) + \sigma_{0,1}(h_{\mathrm{sig}}, h_{\mathrm{int}})}, \tag{6}$$

where $i_{d_{\mathrm{sig}},d_{\mathrm{int}}}(h_{\mathrm{sig}}, h_{\mathrm{int}}) = i_{d_{\mathrm{sig}}}(h_{\mathrm{sig}}) + i_{d_{\mathrm{int}}}(h_{\mathrm{int}})$ is the resulting signal ($d_{\mathrm{sig}} = 0$ or 1) and interferer ($d_{\mathrm{int}} = 0$ or 1) current at the decision circuit, $i_{d_{\mathrm{sig}}}(h_{\mathrm{sig}}) = a_{d_{\mathrm{sig}}} R P_{R,\mathrm{sig}}(h_{\mathrm{sig}})$ is the signal current for data 1 and 0, and $i_{d_{\mathrm{int}}}(h_{\mathrm{int}}) = a_{d_{\mathrm{int}}} R P_{R,\mathrm{int}}(h_{\mathrm{int}})$ is the interferer current for data 1 and 0. $P_{R,\mathrm{sig}}$ and $P_{R,\mathrm{int}}$ are respectively the instantaneous received signal and interferer average powers. Also, $a_0 = 2/(r+1)$, $a_1 = 2r/(r+1)$, r is the extinction ratio (assumed identical for signal and crosstalk), $R = \eta q/E$ is

the responsivity (in A/W), q is the electron charge, $E = hf_c$ is the photon energy (corresponding signal and interferer values differ slightly), and h is Planck's constant. The factor ¼ in Eq. (5) replaces the usual ½ due to the negligible impact of errors on signal 1, interferer 1 and signal 0, interferer 0 combinations.

The total OLT receiver noise variance $\sigma^2_{d_{\text{sig}},d_{\text{int}}}$ is the summation of the signal shot noise, ASE shot noise, signal-ASE beat noise, and ASE–ASE beat noise variances, given respectively in Eqs. (7)–(10), plus the thermal noise variance σ^2_{th}:

$$\sigma^2_{\text{shot}\_d_{\text{sig}},d_{\text{int}}} = 2qi_{d_{\text{sig}},d_{\text{int}}}(h_{\text{sig}},h_{\text{int}})B_e, \tag{7}$$

$$\sigma^2_{\text{shot,ASE}} = 2m_tB_0N_0qRB_e, \tag{8}$$

$$\sigma^2_{\text{sig}\_d_{\text{sig}},d_{\text{int}}\text{–ASE}} = 4RN_0i_{d_{\text{sig}},d_{\text{int}}}(h_{\text{sig}},h_{\text{int}})B_e, \tag{9}$$

$$\sigma^2_{\text{ASE–ASE}} = 2m_tR^2N_0^2B_0B_e. \tag{10}$$

m_t is the number of polarization states of ASE noise (normally $m_t = 2$), B_0 is the optical bandwidth, and the ASE noise power spectral density (PSD) in a single polarization state at the photodiode is N_0.

V. Turbulence-Accentuated Crosstalk

To develop insight into system behavior, it is useful to first consider the case where the signal experiences turbulence but the interferer does not. To do so Eqs. (4)–(10) are used in an optically preamplified case [gain G, ASE PSD at amplifier output is $N_0 = 0.5(NFG-1)E$] and with no amplifier ($G = 1$). Then, $P_{R,\text{sig}}(h_{\text{sig}}) = GP_{\text{inst,sig}}(h_{\text{sig}})$, where $P_{\text{inst,sig}}(h_{\text{sig}})$ is the instantaneous received signal power and thus $P_{\text{inst,sig}}(1)$ is also the turbulence-free average received power of the signal at the preamplifier input. $P_{R,\text{int}} = GP_{\text{int}}$ is fixed by setting a signal-to-crosstalk ratio $C_{\text{XT}} = P_{R,\text{sig}}(1)/P_{\text{int}}$, where P_{int} is the crosstalk power (which, in this case, is not turbulence affected).

The other case of interest is where the interferer experiences turbulence, but not the signal. Then $P_{R,\text{int}}(h_{\text{int}}) = GP_{\text{inst,int}}(h_{\text{int}})$, where $P_{\text{inst,int}}(h_{\text{int}})$ is the instantaneous received interferer power, $P_{R,\text{sig}} = GP_{\text{sig}}$ is fixed by setting a signal-to-crosstalk ratio $C_{\text{XT}} = P_{\text{sig}}/P_{R,\text{int}}(1)$, where $P_{R,\text{int}}(1)$ is also the turbulence free average received interferer power at the preamplifier input, and P_{sig} is the (nonturbulent) signal power.

A. Example Results

BER versus average received signal power results, focusing on turbulence accentuation of interchannel crosstalk, now follow. The parameters used are as follows: laser wavelength $\lambda = 1.55$ μm, data rate $R_b = 2.5$ Gbps, extinction ratio $r = 10$ dB, optical bandwidth $B_0 = 60$ GHz, quantum efficiency $\eta = 0.8$, amplifier noise figure NF = 4.77 dB, and gain $G = 30$ dB. The thermal noise current is taken as 7×10^{-7} A, corresponding to an unamplified receiver with −23 dBm sensitivity at a BER of 10^{-12} [8]. The weak turbulence (WT) and strong turbulence (ST) conditions for FSO link length $l = 1000$ m come from $C_n^2 = 8.4 \times 10^{-15}$ m$^{-2/3}$ and $C_n^2 = 1 \times 10^{-13}$ m$^{-2/3}$, respectively. Results are presented for 1) no interferer, no turbulence (S); 2) signal with interferer, no turbulence (S,XT); 3) signal with turbulence, no interferer (turbS); 4) signal with turbulence, interferer with no turbulence (turbS,XT); and 5) signal with no turbulence, interferer with turbulence (S,turbXT) cases.

It can be seen from the results [Fig. 2 (nonamplified case) and Fig. 3 (optically preamplified case)] that the turbulence accentuation of crosstalk introduces BER floors that rise with turbulence strength. In the WT cases, floors occur at much lower BERs than the range given, using signal-to-crosstalk ratios of 30 and 15 dB. In the ST cases the turbS,XT BER floors when $C_{\text{XT}} = 30$ dB, while the turbS,XT and S,turbXT both floor when $C_{\text{XT}} = 15$ dB (the former more significantly).

To understand turbulence accentuation of crosstalk, consider first the S,turbXT case and note that turbulent crosstalk can sometimes increase its 1 value so that {data 0, crosstalk 1} is greater than {data 1, crosstalk 0} (neglecting receiver noises). This applies when h_{int} is high enough,

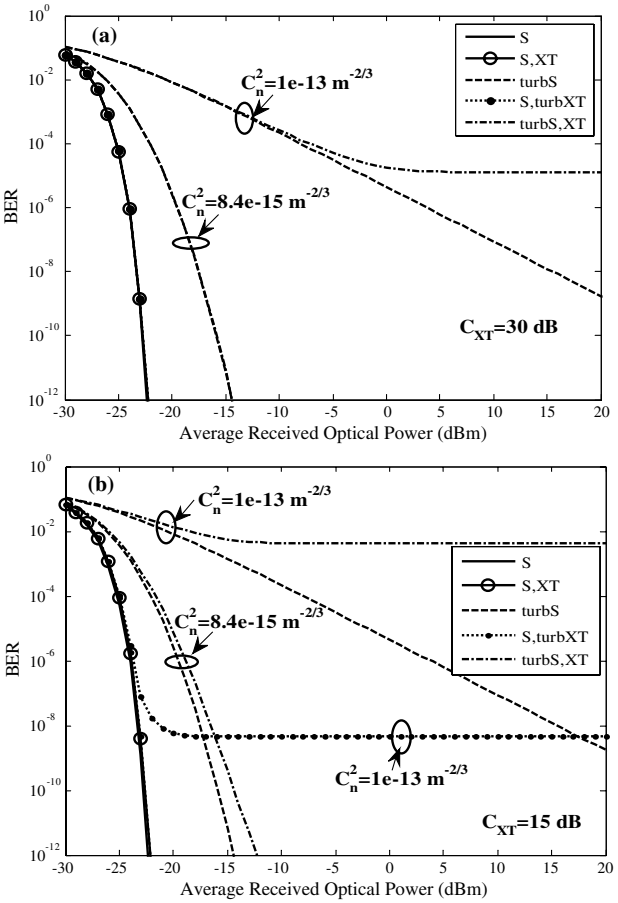

Fig. 2. BER versus average received signal optical power (dBm) for WT and ST (no amplifier): (a) $C_{\text{XT}} = 30$ dB and (b) $C_{\text{XT}} = 15$ dB.

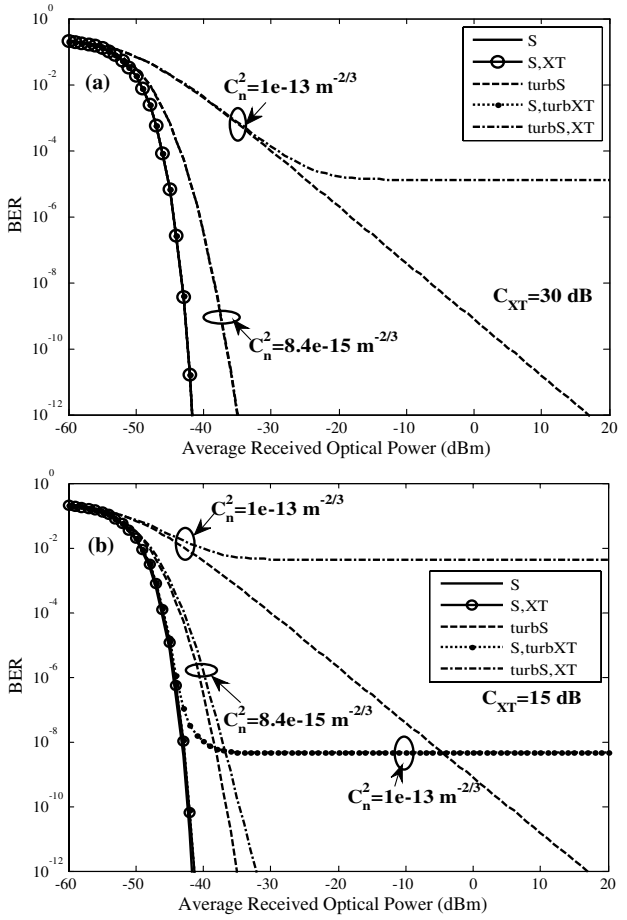

Fig. 3. BER versus average received signal optical power (dBm) for WT and ST ($G = 30$ dB): (a) $C_{XT} = 30$ dB and (b) $C_{XT} = 15$ dB.

and when it is (as when the data rate is much faster than the turbulence), it effectively holds this value long enough for the threshold to adapt and be set above the {data 1, crosstalk 0} value but below {data 0, crosstalk 1} value, inevitably leading to errors (except when receiver noises operate to correct them). This occurs when $h_{\text{int}} > C_{\text{XT}}$, so integrating this tail of the crosstalk's turbulence pdf sets the error floor. The floor starts once the signal power and crosstalk are sufficiently large that the noises are very unlikely to cause a reverse threshold crossing. Similar arguments apply for the turbS,XT case, except this time there comes a point, by attenuating the signal, where {data 1, crosstalk 0} is brought lower than {data 0, crosstalk 1}, again neglecting receiver noises and leading to a threshold set below {data 0, crosstalk 1} and above {data 1, crosstalk 0}. This occurs when $h_{\text{sig}} < 1/C_{\text{XT}}$, setting the error floor value via integration of the signal's turbulence pdf.

VI. BER Evaluation for Hybrid WDM PON FSO System

A. Upstream Transmission

Equations (4)–(10) can now be used for the specific system calculations that follow. The single crosstalk is relevant where a dominant interferer exists (e.g., in some sparsely populated dense wavelength division multiplexing grids or where particular interferer transmitters are higher powered). There is also the possibility of schemes where some distribution links are fiber and some are FSO. Now the average received optical power values at the OLT photodiode for the desired signal and interferer are given, respectively, as

$$P_{R,\text{sig}}(h_{\text{sig}}) = GP_{u_{T,\text{sig}}} h_{\text{sig}} L_{\text{fso,sig}} L_{\text{bs,sig}} L_{c,\text{sig}} L_{\text{mux}} L_{\text{fiber}} L_{\text{demux}}, \tag{11}$$

$$P_{R,\text{int}}(h_{\text{int}}) = GP_{u_{T,\text{int}}} h_{\text{int}} L_{\text{fso,int}} L_{\text{bs,int}} L_{c,\text{int}} \times L_{\text{mux}} L_{\text{fiber}} L_{\text{demux}} L_{\text{demux,XT}}, \tag{12}$$

where $L_{\text{demux,XT}}$ is the additional loss (above L_{demux}) the interferer has when coupled onto the signal photodiode by the demux. $P_{u_{T,\text{sig}}}$ and $P_{u_{T,\text{int}}}$ are respectively the signal and interferer ONU transmit powers. In principle, these could be allowed to differ under a power control algorithm. $L_{\text{fso}} = 10^{(-\alpha_{\text{fso}} l_{\text{fso}}/10)}$ is the atmospheric loss (α_{fso} in dB/km), and $L_{\text{fiber}} = 10^{(-\alpha_{\text{fiber}} l_{\text{fiber}}/10)}$ is the fiber loss (α_{fiber} in dB/km). The loss due to beam spreading L_{bs} in the FSO link, for signal and interferer, comes from [3,14]

$$L_{\text{bs}} = \left(\frac{D_{RX}}{\theta l_{\text{fso}}}\right)^2 \tag{13}$$

and can be stated separately for the signal and interferer.

Under the assumption that the end facet of the short single mode fiber leading to the mux is positioned in the focal plane of the RCL, the coupling loss for the signal and interferer can be calculated from [37]

$$L_c = 1 - \left\{ 8a^2 \int_0^1 \int_0^1 \left(\begin{array}{l} \exp\left[-\left(a^2 + \frac{A_{RX}}{A_C}\right)(x_1^2 + x_2^2)\right] \\ \times I_0\left(2\frac{A_{RX}}{A_C} x_1 x_2\right) x_1 x_2 \end{array} \right) \mathrm{d}x_1 \mathrm{d}x_2 \right\}, \tag{14}$$

where a is the ratio of the RCL radius to the backpropagated fiber mode radius, $A_{RX} = \pi D_{RX}^2/4$ is the RCL area, $A_C = \pi \rho_C^2$ is the spatial coherence area of the incident plane wave, $\rho_C = (1.46 C_n^2 k^2 l_{\text{fso}})^{-3/5}$ is the spatial coherence radius, and $I_0(\cdot)$ is a modified Bessel function (first kind, zeroth order). Calculations will use $a = 1.12$, which corresponds to the optimum value for a fully coherent incident plane wave.

At the amplifier output the ASE PSD is $N_{0OA} = 0.5(NFG - 1)E$. Different values of N_0 arise depending on the OA position. In the upstream Case A, the received ASE noise PSD can be written as $N_0 = N_{0OA} L_{\text{fiber}} L_{\text{demux}}$, while in Case B, the received ASE noise PSD can be written as $N_0 = N_{0OA} L_{\text{demux}}$.

B. Downstream Transmission

The downstream interchannel crosstalk is not turbulence-accentuated, as (neglecting wavelength difference impact on σ_R^2) it traverses the same atmospheric path as the signal. The downstream BER (conditioned on h_X) (for given fixed transmitter powers for the signal and crosstalk, the dependence on which is omitted below for brevity) is

$$\mathrm{BER}_d(h_X) = \frac{1}{4}\mathrm{erfc}\left(\frac{Q_d(h_X)}{\sqrt{2}}\right), \tag{15}$$

$$Q_d(h_X) = \frac{i_{d_{1,0}}(h_X) - i_{d_{0,1}}(h_X)}{\sigma_{d_{1,0}}(h_X) + \sigma_{d_{0,1}}(h_X)}, \tag{16}$$

where $i_{d_{\mathrm{sig}},d_{\mathrm{int}}}(h_X) = i_{d_{\mathrm{sig}}}(h_X) + i_{d_{\mathrm{int}}}(h_X)$ is the signal ($d_{\mathrm{sig}} = 0, 1$) plus interferer ($d_{\mathrm{int}} = 0, 1$) current at the ONU decision circuit. $i_{d_{\mathrm{sig}}}(h_X) = a_{d_{\mathrm{sig}}} R P_{d_{R_{\mathrm{sig}}}}(h_X)$ and $i_{d_{\mathrm{int}}}(h_X) = a_{d_{\mathrm{int}}} R P_{d_{R_{\mathrm{int}}}}(h_X)$ are the downstream signal and interferer currents.

The average received optical power at the ONU photodiodes for signal and interferer, respectively, are

$$P_{d_{R,\mathrm{sig}}}(h_X) = G P_{d_{T,\mathrm{sig}}} h_X L_{\mathrm{mux}} L_{\mathrm{fiber}} L_{\mathrm{demux}} L_{\mathrm{fso}} L_{\mathrm{bs}}, \tag{17}$$

$$P_{d_{R,\mathrm{int}}}(h_X) = G P_{d_{T,\mathrm{int}}} h_X L_{\mathrm{mux}} L_{\mathrm{fiber}} L_{\mathrm{demux}} L_{\mathrm{demux,XT}} L_{\mathrm{fso}} L_{\mathrm{bs}}, \tag{18}$$

where $P_{d_{T,\mathrm{sig}}}$ and $P_{d_{T,\mathrm{int}}}$ are the respective downstream transmit powers. Equations (7)–(10) may again be used for the electrical domain noises, though the h_X classification as h_{sig} and h_{int} disappears in the downstream.

In the downstream Case A, the effective ASE noise PSD in the single polarization state at the photodiode is given as $N_0 = N_{0OA} L_{\mathrm{demux,sig}} L_{\mathrm{fso,sig}} L_{\mathrm{bs,sig}}$, while in Case B, it is given as $N_0 = N_{0,OA} L_{\mathrm{fiber}} L_{\mathrm{demux,sig}} L_{\mathrm{fso,sig}} L_{\mathrm{bs,sig}}$.

The average downstream BER is given as

$$\overline{\mathrm{BER}_{d,\mathrm{av}}} = \int_0^\infty \mathrm{BER}_d(h_X) p_{\mathrm{GG,sig}}(h_X) \mathrm{d}h_X. \tag{19}$$

VII. Results and Discussion

Results in terms of required optical power are presented to predict the performance for various scenarios of the hybrid WDM network. Turbulent conditions considered are $C_n^2 = 10^{-17}$ m$^{-2/3}$, $C_n^2 = 10^{-15}$ m$^{-2/3}$, and $C_n^2 = 10^{-13}$ m$^{-2/3}$. If the resulting $\sigma_R^2 < 1$, we have WT; if $\sigma_R^2 \approx 1$, we have moderate turbulence; and if $\sigma_R^2 > 1$, we have ST. The required optical power used here is the transmitter power for a BER of 10^{-6}. Much better performance can be achieved with the use of forward error correction (FEC). Note, however, that the precise relationship between the long-time average BER before and after FEC would require FEC to enter the analysis, e.g., within Eq. (4). The main parameters are reported in Table 1; others used will be stated accordingly. Fiber dispersion and nonlinear effects are neglected (for a 20 km feeder, only small penalties would arise). The RCL diameter choice (13 mm) is consistent with the experimental work of [30,38]. Such small-size lenses reduce the possibility of angular misalignment and make practical using small-size-core fiber [38], ensuring compatibility with existing devices and systems.

TABLE I
Key Parameters Used in the Calculation

Parameter	Description	Value
λ_{sig}	Desired signal wavelength	1550 nm
R_b	Data rate	2.5 Gbps
D_{RX}	RCL diameter	13 mm [30,38]
G	Optical amplifier gain	30 dB
NF	Noise figure	4.77 dB
B_0	Demux channel bandwidth	60 GHz
r	Extinction ratio	10 dB (signal and interferer)
l_{fiber}	Feeder fiber length	20 km [1]
l_{fso}	Maximum FSO length	2 km
l_{fiber}	Feeder fiber attenuation	0.2 dB/km [1,2]
l_{fso}	Atmospheric channel attenuation	0.2 dB/km (clear air) [1,12,13]
θ	Transmission divergence angle	0.2 mrad
L_{demux}	Signal mux/demux loss	3.5 dB [1,2,24]
η	Quantum efficiency	0.8

A. Downstream Transmission

Figure 4 shows the downstream required transmitted optical power (dBm) (BER of 10^{-6}) as a function of the FSO link length for the no interferer and single interferer cases, for Case A with signal and crosstalk transmit powers the same. In Fig. 4(a), both the no interferer and single interferer cases have very similar required transmit powers due to the high signal-to-crosstalk ratio (and no turbulence accentuation of crosstalk); however, with a poor demux device ($L_{\mathrm{demux,XT}} = 15$ dB), as shown in Fig. 4(b), the crosstalk effect becomes noticeable, though not dramatically so. Generally as the FSO link length increases, the required optical power increases, since beam spreading loss and scintillation increase, although when $C_n^2 = 10^{-13}$ m$^{-2/3}$, it ultimately tends to flatten off. This is due to the leveling effect occurring when the RCL diameter falls between the spatial coherence radius and the scattering disk [39]. Further, Fig. 4 shows that if the transmitted power can be increased as high as 0 dBm, it can overcome the turbulence effects for all regimes considered except for $C_n^2 = 10^{-13}$ m$^{-2/3}$ and $l_{\mathrm{fso}} > 1200$ m in the single interferer case. From Fig. 4, if the OLT transmitter power is fixed at, say, 0 dBm (to limit fiber nonlinearity), it can be deduced that FSO link lengths of about 1200 m can be used for strong turbulence conditions, in the presence of a single interferer. In Case B (amplifier placed at the OLT transmitter) quite similar results (not shown) are obtained to those in Case A

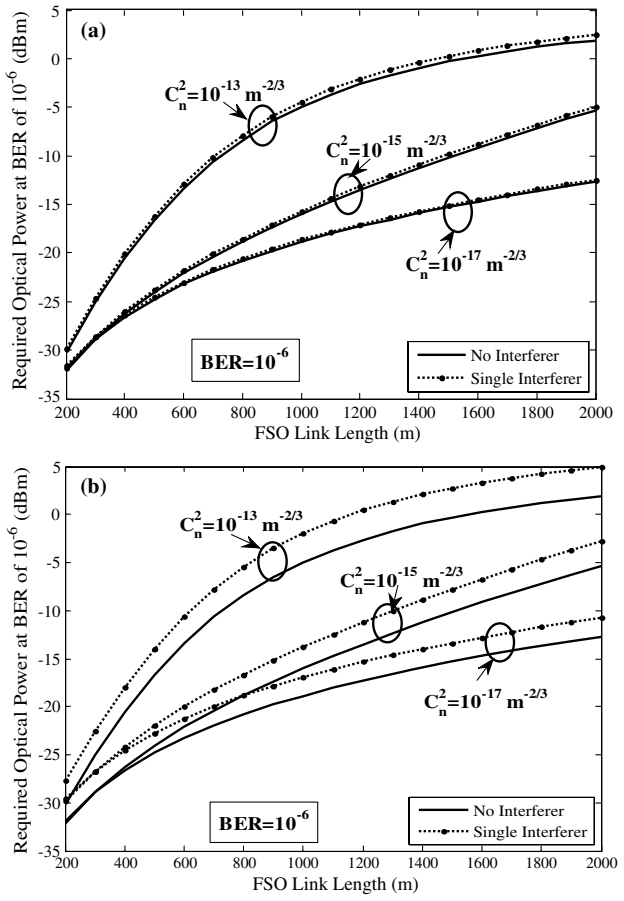

Fig. 4. Downstream required transmitted optical power (dBm) at a target BER of 10^{-6} as a function of the FSO link length (m) for no interferer and single interferer cases, (a) $L_{\text{demux,XT}} = 30$ dB and (b) $L_{\text{demux,XT}} = 15$ dB. The OA was at the remote node (Case A).

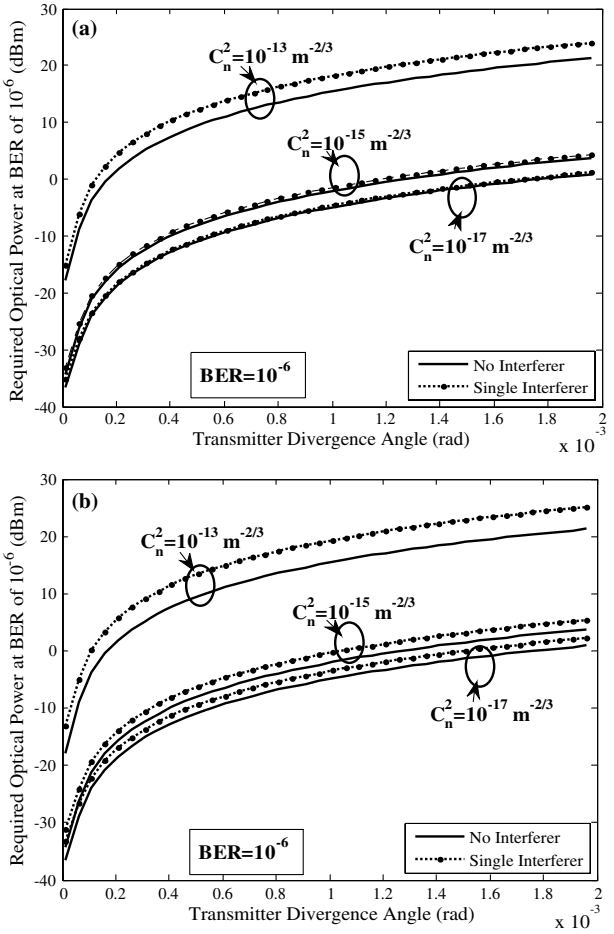

Fig. 5. Downstream required transmitted optical power (dBm) at a target BER of 10^{-6} as a function of the transmitter divergence angle (rad) with $l_{\text{fso}} = 1000$ m for no interferer and single interferer cases, (a) $L_{\text{demux,XT}} = 30$ dB and (b) $L_{\text{demux,XT}} = 15$ dB. The OA was at the remote node (Case A).

above due to the low loss of the fiber. However, the main issue for Case B is the low permitted transmitter power (about −10 dBm [8]) due to fiber nonlinearity issues. Having −10 dBm as the maximum transmitter power will clearly limit the FSO link length.

Figure 5 shows the downstream required transmitted optical power (for BER of 10^{-6}) as a function of the transmitter divergence angle with $l_{\text{fso}} = 1000$ m for no interferer and single interferer cases [Fig. 5(a), $L_{\text{demux,XT}} = 30$ dB, and Fig. 5(b), $L_{\text{demux,XT}} = 15$ dB]. The required optical power clearly increases with the transmit divergence and turbulence strength. Comparing Figs. 5(a) and 5(b) shows the crosstalk impact of a poor demux device. For nontracking systems with relatively large transmit divergence (>1 mrad), more power than in tracking systems will be required. This system type would be required to have greater beam widths in order to compensate for any motions due to building sway. For systems with automatic pointing and tracking, the transmit divergence angle can be narrowed sufficiently (typically with divergence ≪1 mrad), which allows for a secure transmission and larger proportion of transmitted power being collected. Thus the required transmitted power for tracking systems is lower. From Fig. 5, assuming a transmitter power of, say, 0 dBm (possible in Case A), in order to achieve a BER of 10^{-6} and l_{fso} of 1000 m, a small transmit divergence angle (about 0.12 mrad) has to be used, and this can be achieved by using a tracking system. Although tracking helps improve system performance, it also adds considerable cost and complexity to the FSO-based distribution link, particularly if required for each ONU. Tracking systems also have pointing jitter errors [40] not included here. In a nontracking system with single crosstalk (and transmit divergence of 2 mrad), the maximum FSO link length in Case A (maximum transmit power of 0 dBm) is just less than 800 m, while in Case B (with maximum transmit power of −10 dBm) the FSO link length is about 500 m.

B. Upstream Transmission

Figure 6 shows the upstream required transmitted optical power at a target BER of 10^{-6} as a function of the FSO link length with equal signal and interferer FSO link lengths (and transmit powers), $L_{\text{demux,XT}} = 30$ dB, for no interferer and single interferer Case A. On comparing

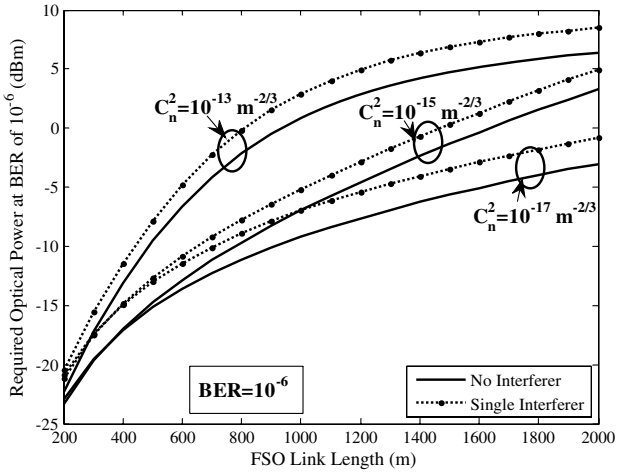

Fig. 6. Upstream required transmitted optical power (dBm) at target BERs of 10^{-6} as a function of the FSO link length (m) for no interferer and single interferer cases, $L_{\text{demux,XT}} = 30$ dB.

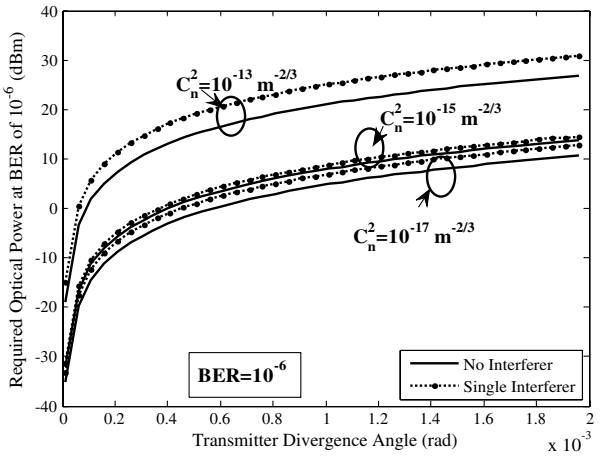

Fig. 7. Upstream required transmitted optical power (dBm) at target BERs of 10^{-6} as a function of the transmitter divergence angle (rad) with $l_{\text{fso}} = 1000$ m for no interferer and single interferer cases, $L_{\text{demux,XT}} = 30$ dB.

the upstream and downstream results (OLT demux loss of 30 dB), i.e., Figs. 6 and 4(a), it can be seen that the required transmit power is higher in the upstream case (Fig. 6) (e.g., by about 6 dB when $C_n^2 = 10^{-13}$ m$^{-2/3}$ and $l_{\text{fso}} = 2000$ m). While turbulence accentuation of crosstalk will occur, it is not the dominant issue here due to the assumption of similar crosstalk and signal powers and lengths. The main factors leading to higher upstream required power are the additional coupling loss via the RCL into fiber that occurs in the upstream (in the downstream we can couple directly onto the photodiode) and the fact that the upstream received OSNR is typically worse. In the upstream, the ONU transmit power can be up to 10 dBm, which fulfils eye-safety conditions for a C-band wavelength range [40]. Therefore, using a reference power of 10 dBm in Fig. 6, it can be seen that an FSO link length of about 2000 m can be used to achieve the target BER value for all atmospheric turbulence conditions with a single interferer.

Figure 7 shows the upstream required transmitted optical power (BER of 10^{-6}) against the transmitter divergence angle for no interferer and single interferer cases with $l_{\text{fso}} = 1000$ m and $L_{\text{demux,XT}} = 30$ dB. As in the downstream [Fig. 5(a)], the required transmitter power increases with transmitter divergence and in the presence of crosstalk, although the required powers are greater in the upstream than the downstream case for similar reasons mentioned earlier (the ASE loss). Using a transmit power of 10 dBm, a tracking system would be required to achieve a small transmit divergence, FSO link length of 1000 m, and BER of 10^{-6} for the whole range of atmospheric turbulence conditions, while in a nontracking system with a divergence of 2 mrad, the maximum FSO link length is about 500 m at a BER of 10^{-6} for an ST condition.

So far it has been assumed that the signal and interferer have identical launch power and distance. The distance requirement is now set aside (but that on launch power retained). Figure 8 shows the upstream required transmitted optical power (BER of 10^{-6}) versus FSO link lengths for signal and interferer for the single interferer case with $L_{\text{demux,XT}} = 15$ dB. It can be seen from Fig. 8 that when the interferer is closer to the remote node than the desired signal, the crosstalk effect becomes more significant and

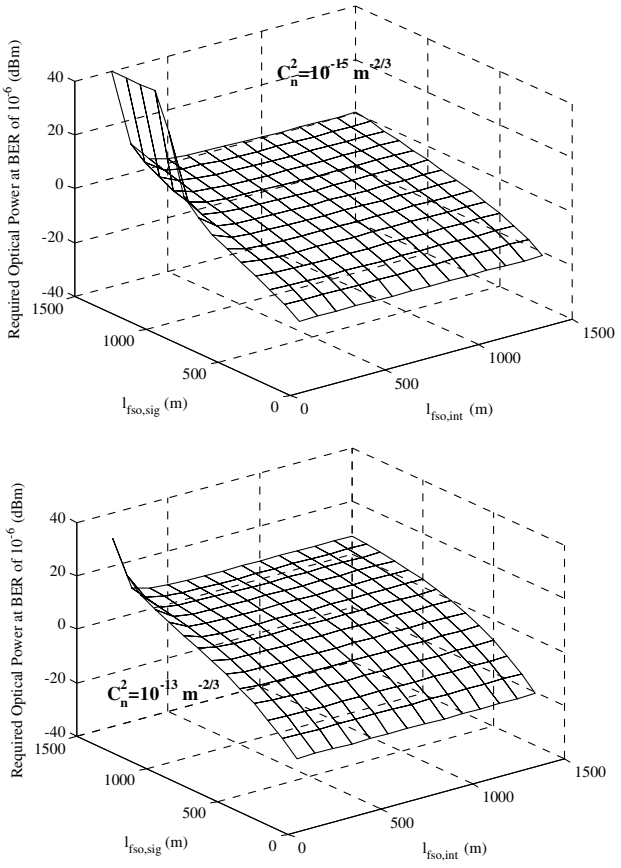

Fig. 8. Upstream required transmitted optical power (dBm) at target BERs of 10^{-6} as a function of the FSO link lengths for signal and interferer (m) for the single interferer case with $L_{\text{demux,XT}} = 15$ dB.

the required transmit power increases. Furthermore, the sudden increase in required power seen on the left of Fig. 8 (for both turbulence strengths considered), i.e., when the FSO link length of the interferer is much closer (less than 200 m) to the remote node and the signal FSO link length is farther away (say about 1500 m), can be related to the same turbulence accentuation effect that led to error floors in the turbS,XT case discussed earlier [see Fig. 3(b)]. In fact, for some FSO link length combinations it is not possible to attain the target BER requirement.

Figure 9 again shows the upstream required transmitted optical power (BER of 10^{-6}) as a function of the FSO link lengths for the signal and single interferer with $L_{\text{demux,XT}} = 15$ dB. However, unlike Fig. 8, now there is assumed a power control algorithm that ensures the average power at the RCL or OLT for each signal is fixed. A similar argument as in Fig. 8 can be established here, but in this case it relates to the turbulence accentuating of the interferer, S,turbXT case (since the effect of turbulence would be greater on the interferer than the desired signal in the regions). Also at some point when $l_{\text{fso,sig}} \ll l_{\text{fso,int}}$, there would be occurrence of an error floor, which restricts the attainment of the target BER. In regions without BER floor effects, this power control approach increases the required optical power to attain the target BERs compared to Fig. 8.

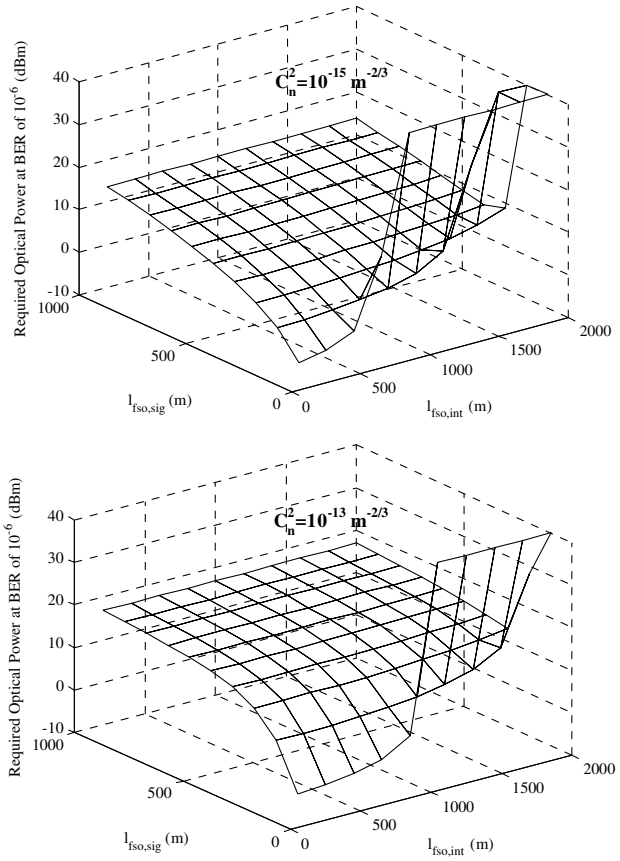

Fig. 9. Upstream required transmitted optical power (dBm) (under the assumption of a power control algorithm that ensures the average power at the RCL or OLT for each signal is fixed) at target BERs of 10^{-6} as a function of the FSO link lengths for signal and interferer (m) for the single interferer case with $L_{\text{demux,XT}} = 15$ dB.

VIII. Conclusion

In this paper, a WDM network incorporating FSO communications for the distribution link has been studied. It can be deduced from this analysis that interchannel crosstalk, turbulence-induced scintillation, and ASE noises are dominant causes of system degradation, especially in the upstream transmission, causing the BER to increase by several orders of magnitude. The results obtained indicate that in a clear atmosphere with a sufficiently high signal-to-crosstalk ratio, the proposed system can achieve human-safe and high-capacity access networks. The location of the OA will make little difference to the performance calculations in both directions, but the issue of capping of the fiber launch power is significant in the downstream. Finally, the OA positioning would also depend on other design considerations, such as fiber nonlinearity and powering of a pointing and tracking system at the remote node.

References

[1] C. H. Lee, W. V. Sorin, and B. Y. Kim, "Fiber to the home using a PON infrastructure," *J. Lightwave Technol.*, vol. 24, pp. 4568–4583, 2006.

[2] J. Prat, *Next-Generation FTTH Passive Optical Networks: Research Towards Unlimited Bandwidth Access*. Springer, 2008.

[3] S. Bloom, E. Korevaar, J. Schuster, and H. A. Willebrand, "Understanding the performance of free-space optics," *J. Opt. Netw.*, vol. 2, pp. 178–200, June 2003.

[4] D. O. Caplan, "Laser communication transmitter and receiver design," *J. Opt. Fiber Commun. Rep.*, vol. 4, pp. 225–362, 2007.

[5] T. H. Carbonneau and D. R. Wisely, "Opportunities and challenges for optical wireless: the competitive advantage of free space telecommunications links in today's crowded marketplace," *Proc. SPIE*, vol. 3232, pp. 119–128, Jan. 1998.

[6] D. Killinger, "Free space optics for laser communication through the air," *Opt. Photon. News*, vol. 13, no. 10, pp. 36–42, Oct. 2002.

[7] S. Karp, R. M. Gagliardi, S. E. Moran, and L. B. Stotts, *Optical Channels: Fibers, Clouds, Water and the Atmosphere*. New York: Plenum, 1988.

[8] R. Ramaswami and K. N. Sivarajan, *Optical Networks—A Pratical Perspective*, 2nd ed. London: Academic, 2002.

[9] R. P. Davey, D. B. Grossman, M. Rasztovits-Wiech, D. B. Payne, D. Nesset, A. E. Kelly, A. Rafel, S. Appathurai, and S. Yang, "Long-reach passive optical networks," *J. Lightwave Technol.*, vol. 27, pp. 273–291, Feb. 2009.

[10] E. Ciaramella, Y. Arimoto, G. Contestabile, M. Presi, A. D'Errico, V. Guarino, and M. Matsumoto, "1.28 terabit/s (32 × 40 Gbit/s) WDM transmission system for free space optical communications," *IEEE J. Sel. Areas Commun.*, vol. 27, pp. 1639–1645, 2009.

[11] L. Kazovsky, S.-W. Wong, T. Ayhan, K. M. Albeyoglu, M. R. N. Ribeiro, and A. Shastri, "Hybrid optical wireless access networks," *Proc. IEEE*, vol. 100, pp. 1197–1225, 2012.

[12] E. S. Son, K. H. Han, J. H. Lee, and Y. C. Chung, "Survivable network architectures for WDM PON," *Optical Fiber Communication Conf. (OFC)*, Anaheim, CA, Mar. 2005, paper OFI4.

[13] E. Leitgeb, M. Gedhart, and U. Birnbacher, "Optical networks, last mile access and applications," *J. Opt. Fiber Commun. Rep.*, vol. 2, pp. 56–85, 2005.

[14] A. K. Majumdar, "Free-space laser communication performance in the atmospheric channel," *J. Opt. Fiber Commun. Rep.*, vol. 2, pp. 345–396, 2005.

[15] J. C. Ricklin, S. M. Hammel, F. D. Eaton, and S. L. Lachinova, "Atmospheric channel effects on free-space laser communication," *J. Opt. Fiber Commun. Rep.*, vol. 3, pp. 111–158, 2006.

[16] H. A. Willebrand and B. S. Ghuman, *Free-Space Optics: Enabling Optical Connectivity in Today's Networks*. Indianapolis, IN: Sams, 2002.

[17] L. C. Andrews and R. L. Phillips, *Laser Beam Propagation Through Random Media*, 2nd ed. Bellingham, WA: SPIE, 2005.

[18] E. Korevaar, I. Kim, and B. McArthur, "Atmospheric propagation characteristics of highest importance to commercial free space optics," *Proc. SPIE*, vol. 4976, pp. 1–12, 2003.

[19] T. Kamalakis, I. Neokosmidis, A. Tsipouras, S. Pantazis, and I. Andrikopoulos, "Hybrid free space optical/millimeter wave outdoor links for broadband wireless access networks," in *IEEE 18th Int. Symp. on Personal, Indoor and Mobile Radio Communications*, Athens, Greece, 2007.

[20] M. Abtahi, P. Lemieux, W. Mathlouthi, and L. A. Rusch, "Suppression of turbulence-induced scintillation in free-space optical communication systems using saturated optical amplifiers," *J. Lightwave Technol.*, vol. 24, pp. 4966–4973, 2006.

[21] A. O. Aladeloba, A. J. Phillips, and M. S. Woolfson, "Improved bit error rate evaluation for optically pre-amplified free-space optical communication systems in turbulent atmosphere," *IET Optoelectron.*, vol. 6, pp. 26–33, Feb. 2012.

[22] M. Razavi and J. H. Shapiro, "Wireless optical communications via diversity reception and optical preamplification," *IEEE Trans. Wireless Commun.*, vol. 4, pp. 975–983, 2005.

[23] A. J. Phillips, J. M. Senior, R. Mercinelli, M. Valvo, P. J. Vetter, C. M. Martin, M. O. Van Deventer, P. Vaes, and X. Z. Qiu, "Redundancy strategies for a high splitting optically amplified passive optical network," *J. Lightwave Technol.*, vol. 19, pp. 137–149, 2001.

[24] I. T. Monroy and E. Tangdiongga, *Crosstalk in WDM Communication Networks*. Norwell, MA: Kluwer Academic, 2002.

[25] D. M. Forin, S. Di Bartolo, G. M. Toshi Beleffi, F. Curti, G. Cincotti, A. Vecchi, S. Ragana, and A. L. J. Teixeira, "Giga Ethernet free-space passive optical networks," *Fiber Integr. Opt.*, vol. 27, pp. 229–236, Apr. 2008.

[26] K. Wang, A. Nirmalathas, C. Lim, and E. Skafidas, "4 × 12.5 Gb/s WDM optical wireless communication system for indoor applications," *J. Lightwave Technol.*, vol. 29, pp. 1988–1996, July 2011.

[27] A. J. Phillips, "Power penalty for burst mode reception in the presence of interchannel crosstalk," *IET Optoelectron.*, vol. 1, pp. 127–134, 2007.

[28] C. X. Yu and D. T. Neilson, "Diffraction-grating-based (de)multiplexer using image plane transformations," *IEEE J. Sel. Top. Quantum Electron.*, vol. 8, pp. 1194–1201, 2002.

[29] S. B. Alexander, *Optical Communication Receiver Design* (SPIE Tutorial Texts in Optical Engineering, Vol. TT22). Bellingham, WA: SPIE, 1997.

[30] F. S. Vetelino, C. Young, L. Andrews, and J. Recolons, "Aperture averaging effects on the probability density of irradiance fluctuations in moderate-to-strong turbulence," *Appl. Opt.*, vol. 46, pp. 2099–2108, Apr. 2007.

[31] "Safety of Laser Products—Part 1: Equipment Classification, Requirements, and User's Guide, New classification standard adopted as of 1 March 2001, Amendment 2," International Electrotechnical Commission, IEC 60825-1, 2001 [Online] Available: http://www.iec.ch/.

[32] N. S. Kopeika and A. Zilberman, "Vertical profiles of aerosol and optical turbulence strength and their effects on atmospheric propagation," *Proc. SPIE*, vol. 3927, pp. 460–467, 2000.

[33] C. Chen, H. Yang, H. Jiang, J. Fan, C. Han, and Y. Ding, "Mitigation of turbulence-induced scintillation noise in free-space optical communication links using Kalman filter," *IEEE Congr. on Image and Signal Processing*, China, Hainan, May 2008, vol. 5, pp. 470–473.

[34] D. J. Wheeler and J. D. Schmidt, "Spatial coherence function of partially coherent Gaussian beams in atmospheric turbulence," *Appl. Opt.*, vol. 50, pp. 3907–3917, 2011.

[35] M. A. Al-Habash, L. C. Andrews, and R. L. Phillips, "Mathematical model for the irradiance probability density function of a laser beam propagating through turbulent media," *Opt. Eng.*, vol. 40, pp. 1554–1562, Aug. 2001.

[36] M. A. Khalighi, N. Schwartz, N. Aitamer, and S. Bourennane, "Fading reduction by aperture averaging and spatial diversity in optical wireless systems," *J. Opt. Commun. Netw.*, vol. 1, pp. 580–593, 2009.

[37] Y. Dikmelik and F. M. Davidson, "Fiber-coupling efficiency for free-space optical communication through atmospheric turbulence," *Appl. Opt.*, vol. 44, pp. 4946–4952, Aug. 2005.

[38] S. Spaunhorst, P. G. LoPresti, S. Pondelik, and H. Refai, "Evaluation of a novel FSO receiver for mitigating alignment errors," *Proc. SPIE*, vol. 7324, 73240H, 2009.

[39] A. O. Aladeloba, A. J. Phillips, and M. S. Woolfson, "Performance evaluation of optically preamplified digital pulse position modulation turbulent free-space optical communication systems," *IET Optoelectron.*, vol. 6, pp. 66–74, Feb. 2012.

[40] A. O. Aladeloba, A. J. Phillips, and M. S. Woolfson, "DPPM FSO communication systems impaired by turbulence, pointing error and ASE noise," in *14th Int. Conf. on Transparent Optical Networks (ICTON)*, Coventry, UK, 2012.

Abisayo O. Aladeloba (S'11) received a bachelor's degree in physics from the Federal University of Technology, Akure, Nigeria, in 2006. He received an M.Sc. degree in electronic, communications, and computer engineering from the University of Nottingham, UK, in 2009, where he is currently working toward a Ph.D. degree. His research interests are in wireless optical communication, modulation techniques for free-space optical communication systems, optical amplifiers, optical performance, and direct detection receiver modeling.

Malcolm S. Woolfson graduated in 1978 with a B.Sc. in mathematics and physics from the University of Bristol. Between 1978 and 1981 he was a research student in the Department of Physics at the University of Warwick, where he worked in the area of surface physics; he was awarded a Ph.D. degree in 1982. Between 1981 and 1983 he was employed as a Research Assistant in the Department of Physics at the University of Sheffield, where he carried out research into the dynamics of atoms in liquids. In 1983 he joined the Marconi Research Centre in Chelmsford, where he worked in the area of signal and data processing techniques for tracking radar. Since 1987 he has been a Lecturer in Signal Processing in the Department of Electrical and Electronic Engineering at the University of Nottingham. He has been involved in the application of a variety of signal and image processing techniques to various areas of engineering.

Andrew J. Phillips obtained his B.Sc. (Hons.) in mathematics from the University of Manchester in 1990, his M.Sc. in applied optics from the University of Salford in 1992, and his Ph.D. in optical communications from Manchester Metropolitan University (MMU) in 1995. He undertook postdoctoral work at MMU between 1995 and 2000, including work on the EU ACTS-PLANET project, and joined Marconi Communications in 2000. He took up his present post at the University of Nottingham as Lecturer in Photonic Communications Technology in January 2003. His research interests include optical amplification, regeneration, optical access, free-space optical communication, optical performance monitoring, and BER evaluation. He has published over 70 papers in journals and conferences. Dr. Phillips is a Member of the Institution of Engineering and Technology.